



**HAL**  
open science

## Decreased spontaneous electrical activity in neuronal networks exposed to radiofrequency 1800 MHz signals

Corinne El Khoueiry, Daniela Moretti, Rémy Renom, Francesca Camera, Rosa Orlacchio, André Garenne, Florence Poullétier de Gannes, Emmanuelle Poque-Haro, Isabelle Lagroye, Bernard Veyret, et al.

### ► To cite this version:

Corinne El Khoueiry, Daniela Moretti, Rémy Renom, Francesca Camera, Rosa Orlacchio, et al.. Decreased spontaneous electrical activity in neuronal networks exposed to radiofrequency 1800 MHz signals. *Journal of Neurophysiology*, 2018, 120 (6), pp.2719-2729. 10.1152/jn.00589.2017. hal-01943451

**HAL Id: hal-01943451**

**<https://inria.hal.science/hal-01943451>**

Submitted on 17 Dec 2018

**HAL** is a multi-disciplinary open access archive for the deposit and dissemination of scientific research documents, whether they are published or not. The documents may come from teaching and research institutions in France or abroad, or from public or private research centers.

L'archive ouverte pluridisciplinaire **HAL**, est destinée au dépôt et à la diffusion de documents scientifiques de niveau recherche, publiés ou non, émanant des établissements d'enseignement et de recherche français ou étrangers, des laboratoires publics ou privés.

1 **DECREASED SPONTANEOUS ELECTRICAL ACTIVITY IN NEURONAL**  
2 **NETWORKS EXPOSED TO RADIOFREQUENCY 1800 MHZ SIGNALS**

3

4 Corinne El Khoueiry<sup>1</sup>, Daniela Moretti<sup>2</sup>, Rémy Renom<sup>1</sup>, Francesca Camera<sup>3</sup>, Rosa Orlacchio<sup>4</sup>, André  
5 Garenne<sup>5</sup>, Florence Poulletier De Gannes<sup>1</sup>, Emmanuelle Poque-Haro<sup>1</sup>, Isabelle Lagroye<sup>1,6</sup>, Bernard  
6 Veyret<sup>1,6</sup> and Noëlle Lewis<sup>1</sup>

7

8 <sup>1</sup> University of Bordeaux, CNRS, IMS, UMR 5218, Talence, France

9 <sup>2</sup> Center of Synaptic Neuroscience and Technology, IIT, Genoa, Italy

10 <sup>3</sup> La Sapienza University, DIET, Rome, Italy

11 <sup>4</sup> University of Rennes 1, IETR, Rennes, France

12 <sup>5</sup> University of Bordeaux, CNRS, IMN, UMR 5293, Bordeaux, France

13 <sup>6</sup> Paris "Sciences et Lettres" Research University, Paris, France

14

15 **CORRESPONDENCE:**

16 Noëlle Lewis

17 Email: noelle.lewis@u-bordeaux.fr

18 IMS Laboratory, University of Bordeaux

19 351 Cours de la Libération

20 33405 Talence cedex, France

21 **ABSTRACT**

22 So far, the only identified biological effects of radiofrequency fields (RF) are known to be caused by  
23 heating but the issue of potential nonthermal biological effects, especially on the central nervous  
24 system (CNS), remains open. We previously reported a decrease in the firing and bursting rates of  
25 neuronal cultures exposed to a Global System for Mobile (GSM) RF field at 1800 MHz for 3 min  
26 (Moretti et al. 2013). The aim of the present work was to assess the dose-response relationship for  
27 this effect, and also identify a potential differential response elicited by pulse-modulated GSM and  
28 continuous-wave (CW) RF fields. Spontaneous bursting activity of neuronal cultures from rat  
29 embryonic cortices was recorded using 60-electrode Multi Electrode Arrays (MEAs). At 17-28 days *in*  
30 *vitro*, the neuronal cultures were subjected to 15-min RF exposures, at SARs (Specific Absorption  
31 Rates) ranging from 0.01 to 9.2 W/kg. Both GSM and CW signals elicited a clear decrease in bursting  
32 rate during the RF exposure phase. This effect became more marked with increasing SAR and lasted  
33 even beyond the end of exposure for the highest SAR levels. Moreover, the amplitude of the effect  
34 was greater with the GSM signal. Altogether, our experimental findings provide evidence for dose-  
35 dependent effects of RF signals on the bursting rate of neuronal cultures and suggest that part of the  
36 mechanism is nonthermal.

37

38 **Keywords:** *in vitro*; neuronal cultures; radiofrequency fields; GSM-1800 signal; bursting rate.

39

40 **NEW & NOTEWORTHY**

41 In this study, we investigated the effects of some RF exposure parameters on the electrical activity of  
42 neuronal cultures. We detected a clear decrease in bursting activity, dependent on exposure duration.  
43 The amplitude of this effect increased with the SAR level and was greater with GSM than with CW  
44 signal, at the same average SAR. Our experiment provides unique evidence of a decrease in  
45 electrical activity of cortical neuronal cultures during RF exposure.

**46 INTRODUCTION**

47 The rapid development of wireless communications has raised questions about potential increased  
48 health risks related to exposure to radiofrequency fields (RF). The close proximity between the mobile  
49 phone and the brain of the user, combined with the fact that neurons are excitable cells, make the  
50 central nervous system (CNS) a potential target of RF exposure. Absorption of RF fields by biological  
51 tissues is quantified using the Specific Absorption Rate (SAR) metric, expressed in watts per  
52 kilogram (W/kg), which represents the absorbed power per unit of tissue mass. Two types of RF  
53 effects may occur: thermal or nonthermal. The former, which are prominent in case of high-level RF  
54 exposures, are well established and understood, while the latter are still controversial (SCENIHR  
55 2015). In this context, several human electroencephalography (EEG) studies have reported variations  
56 in the EEG power spectrum during and/or after RF exposure, in resting EEG and during sleep (Van  
57 Rongen et al. 2009; SCENIHR 2015), suggesting that RF exposure may directly influence brain  
58 dynamics. However, the mechanisms underlying these effects on the EEG are still unknown.  
59 Therefore, it was deemed necessary to study the spontaneous electrical activity of neuronal networks  
60 *in vitro*, both at cellular and network levels, in order to detect effects of low-level RF on the nervous  
61 system.

62 Our research group previously published an *in vitro* pilot study on neuronal networks exposed to a  
63 Global System for Mobile (GSM) signal at 1800 MHz (Moretti et al. 2013). The GSM signal refers to  
64 the initial development of digital mobile communication systems (2G). It is a TDMA (Time Division  
65 Multiple Access) communication protocol. The pure carrier frequency emission is referred to as CW  
66 (for Continuous Wave) while the GSM signal is a pulsed-modulated signal at 217 Hz with a 1/8 duty  
67 cycle. In that previous study, a novel method was used to record neuronal extracellular electrical  
68 activity under RF exposure. A 30% reversible decrease in firing and bursting rates was found during  
69 3-min GSM 1800 MHz exposures of neuronal cultures from rat embryonic cortices (15-21 days *in*  
70 *vitro*). The reported SAR of 3.2 W/kg was later recalibrated to 4.6 W/kg. To our knowledge, there has  
71 been no new report on exposure in the GHz frequency range of neuronal networks since Moretti et al.  
72 (2013).

73 The research presented here aimed to achieve more precise characterization of the previously  
74 published effect, in terms of dose-effect and potential differential effect between pulsed (GSM) and

75 non-pulsed (CW) RF signals. This involved assessing the amplitude of the effect as a function of  
76 SAR, electric field (E), and RF signal type (i.e. CW or GSM). The effects of all GSM and CW  
77 exposures were compared at the same averaged SAR, so that the total energy transferred to the  
78 sample was identical and the temperature elevation of the culture medium was the same. Data were  
79 also plotted against the averaged E. The exposure protocol consisted of 15-min RF at bulk SARs  
80 ranging from 0.01 to 9.2 W/kg, compared to sham conditions.

81

## 82 **MATERIAL AND METHODS**

### 83 ***Cell culture***

84 To collect electrical activity, primary neurons were cultured on commercial microelectrode arrays  
85 (MEAs) as described previously (Moretti et al. 2013). Polyethyleneimine (PEI) or polylysine (PLL)  
86 (Sigma–Aldrich, St. Quentin-Fallavier, France) were used to coat the active area of the MEA to  
87 promote attachment of neurons in the primary cell culture. These two coating methods have been  
88 tested in order to spread over time the maturity of the neuron cultures, as cultures grown on PEI are  
89 maturing sooner than neurons cultured on PLL. Laminin (Sigma–Aldrich, St. Quentin-Fallavier,  
90 France) was also added on top of the PEI and PLL coatings for better adherence.

91 The primary neuronal cell cultures were obtained from the cortex of embryonic (E18) Sprague–  
92 Dawley rats (Charles River Laboratories, L'Arbresle, France). After 5% isoflurane anesthesia, the  
93 gestating rat was sacrificed by elongation. Embryos cortices were dissected in Dulbecco's Modified  
94 Eagle Medium (DMEM)-penicillin/streptomycin (Fisher Scientific, Illkirch, France), and treated for 30  
95 min with an enzymatic solution containing 20 units/ml of papain and 0.005% of DNase (Worthington  
96 Biochemical Corporation, Lakewood, Colorado, USA). The fragments were then subjected to  
97 mechanical dissociation using a 10-ml serological pipette and centrifuged at 300 g for 5 min at room  
98 temperature. The supernatant was eliminated and the pellet was placed in suspension in a solution  
99 containing DNase. This latter mixture was placed above an albumin-inhibitor solution, to create a  
100 discontinuous density gradient, and then centrifuged at 70 g for 6 min at room temperature. In this last  
101 step, the dissociated cells (in the pellet) were separated from membrane fragments of dead cells in  
102 the supernatant. Finally, the pellet containing cortical cells was suspended in the culture medium

103 composed of neurobasal medium supplemented with 2% B-27, 1% GlutaMAX, and 1%  
104 penicillin/streptomycin (Fisher Scientific, Illkirch, France). Each MEA was plated with a suspension of  
105  $10^5$  cells and kept until recording in a 5% CO<sub>2</sub> incubator at 37 °C in a humidified atmosphere. The  
106 culture medium was changed three times a week.

107

### 108 ***Acquisition system***

109 Neuronal networks were grown in culture chambers that were constituted of a 6 mm-high glass  
110 cylinder sealed with biocompatible silicone on a 60-channel planar MEA from Qwane Biosciences  
111 (Qwane, Lausanne, Switzerland) that was used as electrophysiological interface as previously  
112 described (Moretti et al. 2013). These biochips are built on 15 x 15 mm glass substrates mounted on  
113 printed circuit boards (PCB; 50 x 50 mm) using standard microfabrication technologies. They provide  
114 60 platinum electrodes (200  $\mu$ m spaced with 40  $\mu$ m diameter tips). To allow the insertion of the culture  
115 chamber inside the exposure system, the pre-amplifier (MEA1060-Inv, Multi-Channel Systems (MCS),  
116 Reutlingen, Germany) had to be placed underneath the MEA; we thus had custom MEAs built by  
117 Qwane Biosciences, in which the contact pads were placed on the bottom side of the PCB.

118

### 119 ***Exposure setup and RF signals***

120 The exposure setup for electrophysiological recording comprised the MEA and an open Transverse  
121 ElectroMagnetic cell (TEM), consisting of a rectangular coaxial transmission section tapered towards  
122 the coaxial connectors on both sides, as shown in Fig. 1. A. The inner conductor, or septum, acted as  
123 the positive conductor or hot line. The outer conductor acted as the ground. The impedance along the  
124 TEM cell was 50  $\Omega$ , so a matched 50  $\Omega$  load was placed at the output port. The MEA glass cylindrical  
125 chamber was inserted into the TEM cell through a 14.5 mm-diameter circular hole in the ground plate.  
126 The TEM cell was connected to an RF generator-amplifier as a source of GSM and CW signals at  
127 1800 MHz (RFPA, Artigues-près-Bordeaux, France).

128 RF exposure is characterized by SAR, quantifying the energy deposited in a tissue. SAR, expressed  
129 as W/kg, is the physical quantity that causes tissue heating with RF exposure. In this study, we

130 compared exposure to GSM and CW signals, which have different modulation profiles, as shown in  
 131 Fig. 1. B. The effects of GSM and CW exposure are usually compared at the same time-averaged  
 132 SAR, to ensure the same amount of heating. Due to the pulsed nature of GSM signal, with a 1/8 duty-  
 133 cycle, its peak power SAR is eight times greater than that of the equivalent CW signal (Fig. 1. B).

134

135 Dosimetric modeling of the exposure system that was used in these experiments has been described  
 136 previously (Merla et al. 2011; Moretti et al. 2013). The temperature elevation of the culture medium  
 137 had been measured in the dosimetry study (Merla et al. 2011): it reached 0.6 °C at 15 min, during a  
 138 7.4 W/kg exposure. In our experiments, the medium temperature elevation at a given SAR level was  
 139 estimated from these reference measurements. For example, for a 15-min RF exposure at 9.2 W/kg,  
 140 the temperature increase was estimated at 0.7 °C.

141 To avoid any bias concerning the thermal or non-thermal nature of the mechanism, the dose  
 142 response was plotted as a function of the time-averaged SAR, as well as the time-averaged electric  
 143 field  $E$ . SAR is related to  $E$  as follows:  $SAR = \sigma E^2/\rho$ , where  $\sigma$  is the conductivity of the culture  
 144 medium (2.12 S/m at 1800 MHz; Merla 2011),  $E$  the electric field in V/m and  $\rho$  the density of the  
 145 medium (1000 kg/m<sup>3</sup>). For the CW signal, as the SAR and  $E$  values are constant, the average  $E =$   
 146  $E_{CW} = \sqrt{\rho SAR/\sigma} = 21.7 \sqrt{SAR}$ . Due to the 1/8 duty-cycle for GSM (Fig.1. B), the relationship between  
 147 the average  $E$  of GSM and CW signals with the same average SAR is:  $E_{GSM} = 1/\sqrt{8} E_{CW}$ . SAR and  $E$   
 148 always refer below to time-averaged SAR and  $E$ , respectively.

149

### 150 ***Electrophysiological recordings***

151 In order to maintain the proper cell culture conditions during the recordings, the experiments were  
 152 carried out in a dry incubator (37 °C, 5% CO<sub>2</sub>) where the pre-amplifier, the MEA, and the exposure  
 153 system were placed. The MEA culture chamber was sealed with a removable membrane made of  
 154 fluorinated ethylene-propylene (ALA Scientific Instruments, New York, USA) to prevent evaporation  
 155 while allowing for gas exchange. The pre-amplification gain was 1200 and a shielded cable was used  
 156 to transfer data from the preamplifier, inside the incubator, to a desktop computer equipped with an

157 MCS-dedicated data-acquisition board. Raw data were sampled at 10 kHz/channel. Signals were  
158 recorded and monitored using the MC Rack software (MCS) for on-line visualization and raw-data  
159 storage.

160

### 161 ***Signal Processing and burst detection***

162 The electrical activity of neuronal cultures was analyzed using the SPYCODE software (Bologna et al.  
163 2010). Spiking activity was detected with the differential-threshold precision-timing spike-detection  
164 method (PTSD) (Maccione et al. 2009). It detects a spike when the peak-to-peak amplitude of the  
165 signal exceeds eight times the standard deviation (SD) of the biological noise in a 2 ms sliding  
166 window. The SD of the biological noise was evaluated for each recording channel in the pre-exposure  
167 phase. Then, bursts were detected using the method described by Pasquale et al. (2010). The  
168 algorithm is based on the computation of the logarithmic inter-spike interval (ISI) histogram and  
169 automatically detects the best threshold for distinguishing between inter- and intra-burst ISIs, for each  
170 recording channel of the array. An analog thresholding method was used to detect network bursts,  
171 based on inter-burst interval (IBI) histogram combined with a synchronization criterion implicating a  
172 given amount of the total electrodes (20% generally) (Pasquale et al. 2010).

173 In our previous study (Moretti et al. 2013), several metrics were analyzed: spike firing rate, mean  
174 bursting rate (MBR), duration of bursts, number of bursting channels, network bursts, inter-spike  
175 interval, and inter-burst interval. Since the amplitude of the effect was higher for the MBR, this metric  
176 was used to investigate the role of the various exposure parameters. MBR is the average number of  
177 bursts per minute collected over the burst-active electrodes (defined as yielding at least one burst  
178 during the recording).

179 At the end of the analysis, we extracted raster plots representing spikes, bursts, and network bursts  
180 for each recording, and a visual control was performed for each data file. In total, 17 recordings out of  
181 104 were eliminated from the final results as they exhibited fewer than 10 bursts per minute at the  
182 beginning of the recording (phases S1 and S2).



183 As expected from the dosimetry study (Merla et al. 2011), the electromagnetic field created an  
184 interference on the electrodes, resulting in a recorded artifact during GSM exposure. This artifact, with  
185 the time profile of the GSM 217 Hz modulation, had already been observed and managed in our  
186 previous study (Moretti et al. 2013). Its maximum amplitude was on the order of 1 mV and it had to be  
187 eliminated before spike detection. As explained in (Moretti et al. 2013), we implemented a stop-band  
188 filter to remove it without altering the electrophysiological signal; a set of 30 stop-band filters, each  
189 centered on one artifact harmonic frequency (from 217 Hz to 6510 Hz) was built using Matlab and  
190 integrated in SPYCODE, in the pre-processing section. The impact of this added filter was tested  
191 positively for removing the artifact and preserving the spikes (Moretti et al. 2013). This GSM-filter was  
192 systematically applied to the recorded signals, with or without RF exposure.

193

#### 194 ***Exposure protocol***

195 The neuronal networks were exposed between 17 and 28 days *in vitro* (DIV); in this age range, the  
196 neuronal activity is balanced between random spikes and bursts (Chiappalone et al. 2005; Van Pelt et  
197 al. 2005). In all experiments, after placing the MEA in the recording setup, we waited for the  
198 stabilization of the temperature at 37 °C inside the incubator before starting the recording, in order to  
199 work under standard cell culture conditions.

200 The recording protocol was adapted to assess the dose-response relationship as a function of SAR,  
201 and the potential differential response elicited by pulsed (GSM) and non-pulsed continuous wave  
202 (CW). In this protocol, the exposure phase (E) duration was 15 min, preceded by two “pre-exposure”  
203 phases (non-exposed; S1 and S2) of 15 min each, and followed by two “post-exposure” phases (non-  
204 exposed; P1 and P2) of 15 min each (Fig. 1 C).

205 This protocol lasted 75 min and SARs during the exposure phase ranged from 0.01 to 9.2 W/kg. A  
206 series of sham-exposures was carried out separately, using the same 5-phase protocol but with RF  
207 always OFF, in order to evaluate the baseline activity along this series of phases.

208

#### 209 ***Influence of temperature elevation in the culture medium on burst activity***

210 In our 15-min exposure protocol, the maximal SAR was 9.2 W/kg, which corresponded to a  
211 temperature elevation estimated at 0.7 °C, according to the dosimetry study (Merla et al. 2011). In  
212 order to study the potential effect of bulk heating on neuronal activity, neuron cultures were exposed  
213 during 15 min in the incubator to the heat produced by an electric hotplate (MCS). The temperature  
214 elevation in the culture medium, up to 1 °C, was monitored using a Luxtron probe (LumaSense  
215 Technologies, Erstein, France). The neuronal activity was recorded during the heating phase and the  
216 following 30-min cooling phase. The heating phase started as soon as the electric hotplate was turned  
217 on. The medium temperature reached  $37.80 \pm 0.03$  °C after 5 min and continued increasing gradually,  
218 until it stabilized at 38 °C. After 15-min heat exposure, the hotplate was turned off and the  
219 temperature decreased rapidly to  $37.30 \pm 0.06$  °C after 5 min, then to 37 °C for the rest of the  
220 recording.

221

## 222 ***Statistical analysis and graphs***

223 In order to pool and compare data from different samples, we considered the MBR of the S1 phase as  
224 100%, and we calculated the MBR of the following phases as a percentage of this value. Statistical  
225 analysis was performed using R (R Core Team, 2017) and the PMCMR library (Pohlert, 2014). We  
226 used the Friedman test followed by Conover's multiple comparison test to compare exposure protocol  
227 phases for each group (SHAM, GSM, and CW). Data are presented using whisker box diagrams. A p-  
228 value < 0.05 was considered statistically significant. In the text, data are presented as mean  $\pm$  SEM.  
229 The number of samples (n) used for each analysis is mentioned in the corresponding figure caption.

230

## 231 **RESULTS**

### 232 ***Effect of a 15-min RF exposure at 4.6 W/kg***

233 We first analyzed the effect of 15 min-RF exposure at a SAR of 4.6 W/kg, which was the level of  
234 exposure already used in our previous 3-min GSM exposure experiment (Moretti et al. 2013). In this  
235 15-min exposure protocol, the recordings during the RF exposed phase (E) revealed a clear decrease  
236 in the frequency of spikes and bursts, compared to the pre-exposure recordings of spontaneous

237 neuronal activity (S1, S2), for both GSM and CW signals. Fig. 2 shows a typical recording of the S2,  
238 E, and P1 phases, from a 4.6 W/kg GSM exposed culture; on the raster plots, there was a marked  
239 decrease in electrical activity during the second half of the E phase and it disappeared during the first  
240 minutes of the P1 phase.

241 Given that the total recordings lasted 75 min, sham exposures were performed on 11 cultures in order  
242 to distinguish between variations in spontaneous activity over time and the effects of RF exposure. A  
243 spontaneous decrease of ca. 5 % in MBR was observed in each of the consecutive sham phases,  
244 with a total of  $19.7 \pm 14.9$  % at the end of the 75-min run, but no significant difference was found  
245 within this group ( $p > 0.05$ , Friedman test) (Fig. 3. A). For the RF exposed cultures, the MBR was  
246 corrected by systematically subtracting this average drift from the spontaneous activity in each phase.

247 Figure 3. B-C represents the normalized MBR for 8 GSM- and 6 CW-exposed cultures, at a SAR of  
248 4.6 W/kg. A statistically significant difference was found within the GSM-exposed group ( $p < 0.001$ ).  
249 The MBR for the exposed phase (E) decreased significantly compared to the S1 or S2 phases  
250 ( $p < 0.01$ ). Moreover, the MBR for the P1 and P2 phases were significantly lower than those of the S1  
251 or S2 phases ( $p < 0.001$ ), indicating that burst inhibition was not totally reversible (Fig. 3. B). The result  
252 was similar for CW exposure, with a significant difference within the group ( $p < 0.01$ ). Statistical  
253 analysis revealed that the difference was between the MBR of the E, P1, and P2 phases, compared  
254 to those of the S1 or S2 phases (Fig. 3. C).

255 Given the results of the statistical analysis and the extent of the effect on the E and P1 phases, we  
256 decided to group the MBR of the latter two phases, in order to compare their average MBR with the  
257 average of the S1 and S2 phases. Statistical analysis revealed a highly-significant difference  
258 ( $p < 0.001$ ) between these two groups, but also between average MBR of S1 and S2 compared to that  
259 of P2 (Fig. 3. D, E).

260

261 **Dose response**

262 We then evaluated the dose-effect relationship as a function of SAR in the 0.01 to 9.2 W/kg range,  
 263 with a total of 76 MEA recordings, using both RF signals (CW, n = 35 and GSM, n = 41). Table 1 lists  
 264 the SAR levels used in these experiments.

265 Analysis of the experiments using both signals revealed that burst inhibition was minor and reversible  
 266 at low SAR (ca. 0.1 W/kg), but, at 4.6 W/kg, inhibition was present during the E phase and persisted  
 267 during the P1 phase and, at 9.2 W/kg, bursting activity was completely abolished throughout the E,  
 268 P1, and P2 phases.

269 Given the results of the statistical analysis above, we decided to quantify the decrease in MBR by  
 270 evaluating the  $R_{MBR}$  ratio, comparing averaged MBR for the E and P1 phases with the averaged MBR  
 271 for the S1 and S2 phases,

$$R_{MBR} = 1 - \frac{(MBR_E + MBR_{P1})/2}{(MBR_{S1} + MBR_{S2})/2}$$

272 where  $MBR_{S1}$ ,  $MBR_{S2}$ ,  $MBR_E$ , and  $MBR_{P1}$  are the MBRs during the respective phases. This ratio  
 273 quantifies the relative decrease in MBR observed during (E phase) and after (P1 phase) RF  
 274 exposure, with respect to a reference activity defined by the average MBR in the pre-exposure  
 275 phases (S1 and S2).

276 Figure 4 shows the evolution of  $R_{MBR}$  as a function of SAR, for both signals. The data points were  
 277 fitted using a one-parameter exponential rise function  $R_{MBR} = 1 - \exp(-SAR/(1.44 SAR_{50}))$ , where  
 278  $SAR_{50}$  is the SAR value for  $R_{MBR} = 0.5$  (Fig. 4). We observed that  $R_{MBR}$  increased with SAR for both  
 279 GSM and CW signals. The two fitted curves were similar in shape, and total inhibition was reached at  
 280 SAR ca. 9.2 W/kg for both signals. However, the  $SAR_{50}$  for the GSM signal was 0.56 that of the CW  
 281 signal.

282 The dose response was also plotted as a function of E, the time-averaged electric field (Fig. 5). In this  
 283 case, 100% inhibition was reached at 23 V/m for the GSM signal, compared to 66 V/m for the CW  
 284 signal. When these curves were fitted using the exponential function,  $R_{MBR} = 1 - \exp(-E/(1.44 E_{50}))$ ,  
 285 the fit was much better than in plots versus SAR. The  $E_{50}$  for the GSM signal was 0.29 that of the  
 286 CW signal.

287 Since the neuron cultures were different in terms of age and coating, we investigated the role of these  
288 two parameters in the observed effect. We found no specific distribution of data points according to  
289 age or coating (data not shown), suggesting that the effect depended solely on the exposure  
290 parameters.

291

### 292 ***Influence of temperature elevation in the culture medium on burst activity***

293 Heating by 1 °C caused slight increases in MBR during and after the E phase (Fig. 6.). This indicated  
294 that a temperature elevation at least as large as that obtained at 9.2 W/kg did not cause a decrease in  
295 MBR.

296

## 297 **DISCUSSION**

298 The findings described above confirm our published data on the decrease in burst activity of neuronal  
299 cultures under GSM exposure (Moretti et al. 2013). This previously reported effect was a 30%  
300 reversible decrease in MBR under 3-min GSM exposure at a SAR level of 4.6 W/kg (i.e.  $E =$   
301  $15.9$  V/m). An additional experiment repeating this 3-min exposure protocol for 3 successive times on  
302 16 MEA neuron cultures also showed that this effect was reproducible (Moretti, thesis 2014): the  
303 inhibition of the MBR was of 30%, 41%, and 34% in the first, second, and third exposure phases,  
304 respectively, and this decrease was reversible after each of the three exposure phases. In the present  
305 study, we show that the bursting activity decreased by ca. 75% under 15-min RF exposures at the  
306 same SAR level, and this effect was not immediately reversible, for both GSM and CW signals.  
307 Moreover, at exposure levels ranging from 0.1 to 9.2 W/kg, the decrease in MBR augmented with  
308 increasing SAR (Fig. 4). At 9.2 W/kg ( $E_{CW} = 63.5$  V/m and  $E_{GSM} = 22.5$  V/m), a bulk SAR level at  
309 which the local SAR at the electrodes is ca. 60 W/kg (i.e. 169 V/m) (Merla et al. 2011), bursting was  
310 fully inhibited throughout the exposure and post-exposure phases. The amplitude of the effect did not  
311 depend on the age of the cultures, within the selected two-week range, or the type of coating. The  
312 decrease in bursting rate during the exposure phase and has been replicated over the years by  
313 several experimenters.

314 Altogether, our experimental findings provide evidence that RF signals have significant effects on the  
315 bursting rate of neuronal cultures. The amplitude of these effects was greater under exposure to  
316 pulsed GSM signals:  $SAR_{50\text{ GSM}}/SAR_{50\text{ CW}}$  was 0.56. This was even remarkable when plotted against  
317 the electric field:  $E_{50\text{ GSM}}/E_{50\text{ CW}} = 0.29$ .

318

### 319 **Recorded artifact**

320 As already mentioned in Moretti et al. (2013), an artifact appeared in the recorded signal, only in the  
321 case of GSM exposure, and was properly eliminated by the GSM filter before spike detection.  
322 Nevertheless, we needed to exclude the possibility that this interference was the direct cause of the  
323 effect. RF shielding of the amplifier resulted in a 10-fold decrease in the artifact amplitude, which  
324 suggests that its cause was mainly an interference with the pre-amplification stage. Following that  
325 operation, the artifact was masked in the noise for most electrodes and did not exceed 1 mV at the  
326 maximum SAR level (9.2 W/kg). This maximum voltage of 1 mV is however well below the threshold  
327 needed to stimulate the neurons, i.e. 1 V (Wagenaar et al. 2005; Zrenner et al. 2010). In the case of  
328 CW exposure, the power absorbed on top of the electrode was simulated in Merla et al. 2011:  $SAR_{\text{CW}}$   
329 was ca. 30 W/kg at maximum, corresponding to an electric field  $E_{\text{CW}}$  of ca. 119 V/m. If the relevant  
330 interaction distance of this extracellular electric field with the neuron is ca. 10  $\mu\text{m}$  (i.e., the thickness of  
331 the neuron), this corresponds to a 1 mV RF signal at 1800 MHz. Hence, in both CW and GSM  
332 exposures, the measured or simulated electromagnetic interference with electrodes is not likely to  
333 produce an alteration of the electrophysiological activity of the neuronal network.

334

### 335 **Influence of temperature**

336 It is well known that RF exposure causes temperature elevation, which can lead to biological effects.  
337 The question is whether both thermal and nonthermal mechanisms coexist. We thus investigated the  
338 role of temperature elevation in the elicitation of the effect observed on the neuronal cultures. For that  
339 purpose, we assessed the influence of temperature elevation of the culture medium (ca. 1 °C) on  
340 bursting activity: under those conditions, MBR increased slightly. While causing a similar temperature

341 elevation at 9.2 W/kg, RF exposure had the opposite effect; this implies that the contribution of the RF  
342 nonthermal effect was large enough to revert the heating effect completely.

343

#### 344 **RF effects on *in-vitro* neuronal activity**

345 A very similar experimental approach was recently implemented (Oster et al. 2016), using an open  
346 TEM cell and 60-electrode MEAs. These authors published their first results on cortical neuronal  
347 networks exposed to TETRA (Terrestrial Trunked Radio) pulsed RF signals (Köhler et 2018). The  
348 signal had a carrier frequency of 395 MHz, pulsed at 17.64 Hz. In a series of 15-min TETRA  
349 exposures at 1.17 and 2.21 W/kg, no difference was found in the bursting rate before and after  
350 exposure, while increases in temperature led to an increase in bursting rate, as observed in our work.  
351 The experimental setup was not configured to record electrical activity during the exposure phase,  
352 preventing the authors from observing a potential reversible effect during TETRA exposure.

353 One *in-vitro* investigation assessed the effects of chronic RF exposure (15 min daily for 8 days) on  
354 synaptic function in rat hippocampus cultures, using the patch-clamp technique associated with  
355 immunohistochemistry (Xu et al. 2006). This study revealed that GSM 1800 MHz RF (2.4 W/kg, i.e.  
356 34 V/m) caused a selective decrease in the amplitude of AMPA mEPSCs, but not in their frequency or  
357 decay time, or NMDA current amplitude. Furthermore, the authors reported a decrease in the PSD95-  
358 stained puncta, suggesting a decrease in the density of excitatory synapses after RF exposure. A  
359 parallel study by the same team, focusing on the dendritic development of cultured hippocampal  
360 neurons, also found that the number of spines decreased after the same chronic GSM exposure (Ning  
361 et al, 2007), suggesting that “low-intensity” RF exposure affected the formation of excitatory synapses  
362 in these neurons.

363 Other *in-vitro* investigations have used isolated neurons from ganglionic neuronal networks, a  
364 preparation considerably less complex than the cultured networks used in our experiments and the  
365 studies cited above.

366 Early evidence was published of the effects of RF exposure on the electrical activity of individual  
367 neurons from *Aplysia* ganglia placed within a microwave stripline (Wachtel et al., 1975). Intracellular

368 glass microelectrodes were used to record electrical activity during RF exposure at 1.5 GHz and ca. 1  
369 W/kg, either pulsed (10  $\mu$ s pulses at 1-5 kHz repetition rate) or CW. The largest effect was found with  
370 pacemaker neurons, which were of two types: “beating” pacemakers, with regular inter-spike intervals  
371 (ISI), and “bursting” pacemakers, with an endogenous bursting activity and regular inter-burst  
372 intervals (IBI). RF exposure increased the ISI of “beating” pacemakers, but decreased the IBI of  
373 “bursting” pacemakers. No significant difference was found between pulsed and CW exposure.  
374 Furthermore, qualitative heating tests caused the opposite effects.

375 In a study with a similar design, BP-4 identified neurons isolated from large parietal ganglia of  
376 *Lymnea stagnalis* were exposed in a waveguide at 900 MHz and their spontaneous electrical activity  
377 and ionic currents were recorded (Bolshakov et al., 1992). These pacemaker neurons have a small  
378 number of synaptic inputs and most of them exhibited a steady firing rate under physiological  
379 conditions. However, about 25 percent of the neurons exhibited burst-like transient irregularities. A  
380 conventional microelectrode technique was used to make intracellular recordings. The RF exposure  
381 was pulse-modulated (0.5 to 4 W/kg) or CW (0.5 to 15 W/kg). Exposure to CW RF did not influence  
382 the spontaneous electrical activity of either type of neurons. Pulsed-RF exposures within the same  
383 range of SAR caused specific changes in firing rate, independently of modulation frequency (0.5 to  
384 110 Hz), eliciting a burst within the first minute of a 10 min-exposure in neurons that otherwise  
385 exhibited regular spiking activity. For the second type of neurons, which exhibited spontaneous burst  
386 events, the IBI decreased during exposure. The authors also studied the effect of RF exposure on  
387 ionic currents induced by activating cell-membrane ACh, DA, 5-HT, and GABA receptors and found  
388 no consistent effects. In a previous study (Bolshakov et al., 1986), the authors reported that the firing  
389 rates of *Lymnea* BP-4 neurons decreased during rapid heating and stopped completely at a rate of  
390 0.2 °C/s.

391 These *in-vitro* studies on pacemaker neurons from ganglionic networks revealed an alteration in the  
392 firing patterns of neurons with endogenous firing rhythms and demonstrated that equivalent direct  
393 heating had the opposite effect on firing activity to RF exposure.

394 To investigate the potential mechanisms of RF-induced biological effects, we examined other reports  
395 documenting the effects of millimeter waves (MMW) on neuronal cells. MMW are usually dedicated to  
396 radar or satellite communications and use carrier frequencies in the 30–300 GHz range, i.e. much



397 higher than those of RF mobile phone communications. MMW cannot penetrate deeply into the body,  
398 as they are almost totally absorbed in the superficial layers of the skin within 1 mm of the surface, so  
399 they do not interact with the CNS. Consequently, the studies reported below focused on the potential  
400 effects of MMW on sensory receptors or exploitation of MMW to regulate neuronal activity.

401 Major but reversible electrophysiological effects were reported in patch-clamp experiments where  
402 pyramidal neurons of rat cortical slices were exposed to MMW (Pikov et al, 2010). At power densities  
403 approaching  $1 \mu\text{W}/\text{cm}^2$ , 1-min MMW exposure was accompanied by MMW-induced heating of the  
404 bath solution at  $3 \text{ }^\circ\text{C}$  and produced a considerable decrease in firing during exposure in 4 out of 8  
405 neurons, as well as narrowing the action potential (AP) and decreasing membrane resistance.  
406 However, these effects were considerably more marked than those induced by  $10^\circ\text{C}$  general bath  
407 heating (Lee et al, 2005), indicating that MMW-induced effects could not be entirely attributed to  
408 heating. Moreover, blocking the intracellular  $\text{Ca}^{2+}$ -mediated signaling did not significantly alter the  
409 MMW-induced neuronal response, suggesting that MMW interact directly with the neuronal plasma  
410 membrane. This hypothesis was further examined in a second study performed by the same group,  
411 where the physiological effects of low-intensity 60 GHz RF on individual neurons in the Leech ganglia  
412 were investigated using a standard sharp-electrode electrophysiology setup (Romanenko et al, 2014).  
413 The neurons exhibited spontaneous, network-based firing activity, maintained by multiple reciprocal  
414 inhibitory and excitatory loops. During a 1-min RF exposure (incident power densities: 1, 2, and  
415  $4 \text{ mW}/\text{cm}^2$ ) or gradual bulk heating at a rate of  $0.04 \text{ }^\circ\text{C}/\text{s}$ , the neurons exhibited a similar dose-  
416 dependent hyperpolarization of the plasma membrane and decrease in AP amplitude. However, a  
417 major difference between the effects of MMW exposure and bath heating was that the firing rate was  
418 suppressed at all MMW power densities, but increased in a dose-dependent manner during gradual  
419 bath heating. Moreover, narrowing of the AP half-width during MMW irradiation at  $4 \text{ mW}/\text{cm}^2$  was 5  
420 times more pronounced than during equivalent bath heating. The mechanism underlying these effects  
421 was hypothesized to involve specific coupling of MMW energy with the neuronal plasma membrane.  
422 These two *in-vitro* studies revealed that, at relatively low power exposure levels, MMW exposure  
423 modulated electrophysiological activity by decreasing or suppressing AP firing rate, in a manner  
424 similar to that found in our investigation. In another study, the same group showed that pulsed  
425 60 GHz-MMW, with a modulation frequency between 3 and 20 Hz and a power of 64 to 550 mW,  
426 altered the spontaneous electrical activity of Leech ganglia (Romanenko et al. 2016), while the

427 resulting temperature elevation was, in this case, negligible (under 0.1 °C). The effects on AP were  
428 somewhat similar to those reported in their previous study, using continuous MMW (Romanenko et al.  
429 2014): a decrease in amplitude, half-width, depolarization, and repolarization phases, reinforcing their  
430 hypothesis that MMW interacted with the plasma membrane. This conclusion was also reached over  
431 the years by the Ramundo-Orlando group who suggested that MMW affected membrane proteins and  
432 phospholipid organization in the bilayer, where water molecules seem to play an important role  
433 (Ramundo-Orlando, 2010).

434 *In-vitro* studies investigating the effects of RF exposure on neural cells and network firing activity  
435 suggested interaction mechanisms with either the plasma membrane or synapses. However, some  
436 authors published critical review of nonthermal models of interaction mechanisms, examining the  
437 effects produced directly by the applied fields (Foster, 2000 ; Apollonio 2013); they concluded that  
438 there were no plausible mechanisms for nonthermal effects. Experimentally, the existence of  
439 nonthermal effect can be investigated by comparing the RF effects to the effects of equivalent direct  
440 heating or by comparing pulsed and non-pulsed RF exposures, at the same time-averaged SAR  
441 (Pickard et al. 1981). In the studies cited above, the results of multiple comparisons suggested that  
442 some of the RF-induced effects were not entirely thermal.

443

#### 444 **RF GSM/CW differential effects on EEG**

445 In terms of potential RF effects on the CNS, numerous studies have revealed differential effects  
446 between pulsed and continuous RF on the electroencephalogram (EEG). An extensive review has  
447 concluded that such differential effects mainly affect the CNS (Juutilainen et al. 2011). Indeed, a  
448 number of experimental studies (human or *in vivo*) seem to have given evidence for effects of pulsed  
449 RF versus non-pulsed RF on the EEG, as developed hereafter.

450 RF experiments on the human nervous system have focused on cognitive function, sleep, and EEG.  
451 A thorough review of the literature yielded many reports of effects caused by exposure to RF signals  
452 of various types. EEG experiments have adopted three approaches: 1) resting EEG, 2) EEG during  
453 the various sleep phases, and 3) evoked potentials, corresponding to changes in electrical potential  
454 generated by the nervous system in response to external stimulation, or sensory or cognitive activity,

455 observable on the EEG recording. Many articles have been published on the effects of mobile  
456 telephony-related RF on human sleep and EEG (Kwon and Hämäläinen, 2011; reviewed in Regel et  
457 al. 2007; SCENIHR 2015). From the published literature, it may be concluded that: 1) no effect on  
458 cognitive function and hearing has been established, 2) effects on sleep have been reported but are  
459 not fully consistent among research groups, and 3) some studies have shown effects of pulsed, but  
460 not non-pulsed (CW) signals on the spectrum of EEG.

461 In a study of the effect of RF on spindles during sleep (Schmid et al. 2012), 30 volunteers were  
462 exposed to a 900 MHz signal, pulsed at 14 or 217 Hz for 30 min before they went to sleep. Exposure  
463 to 14 Hz significantly increased the contribution of spindles during non-REM sleep, while only a slight  
464 trend was observed at 217 Hz. These results were confirmed in a study in which 20 volunteers were  
465 exposed to a 900 MHz GSM signal at 0.6 W/kg (Loughran et al. 2012). The EEG spectral power was  
466 increased in the spindle range during non-REM sleep. In another sleep study conducted on 16  
467 volunteers exposed to a pulsed RF signal at 0.8 Hz (Lustenberger et al. 2013), observation of the  
468 effects of RF on slow-wave activity revealed an increase following exposure to the pulsed RF signal,  
469 but not to CW. Spindle activity was not affected. Furthermore, the EEG of 72 wakeful volunteers  
470 exposed sequentially to a GSM (average SAR 0.06 W/kg) or CW (average SAR 1.95 W/kg) signal  
471 was assessed; GSM exposure caused a weakening of the alpha band, while CW was as effective as  
472 the pulsed signals (Perentos et al. 2013).

473 In other reports, the comparison was not possible between pulsed and non-pulsed signals. For  
474 example, 26-min 0.49 W/kg GSM exposures caused statistically significant decreases in the alpha  
475 band spectral power under closed-eyes conditions (Ghosn et al. 2015). There was no effect of 30-  
476 min, ca. 1.75 W/kg UMTS exposure, in a study on the EEG spectral power in any of the delta, theta,  
477 alpha, and beta frequency bands (Trunk et al. 2013). In a recent report, the newly deployed LTE  
478 signal (4G) was used to expose human volunteers and assess the effects on EEG. Exposure at  
479 2.61 GHz and 1.34 W/kg (over 10 g of tissue) reduced the spectral power and the interhemispheric  
480 coherence in the alpha and beta bands of the frontal and temporal brain regions (Yang et al. 2016).  
481 Hinrikus et al. (2016) confirmed its previous work giving evidence of effects on the EEG spectrum in  
482 volunteers exposed to 450 MHz RF amplitude modulated at 7, 40, and 1000 Hz (peak SAR of  
483 0.3 W/kg over 1 g). The authors made some hypotheses about the mechanism based on an

484 increased fluidity of water under RF exposure coupled with parametric excitation of some brain  
485 bioelectric processes. Independent replication and further experimental evidence will be needed to  
486 test this hypothesis.

487 There have been a few reports of effects of RF exposure on the nervous system of rats. Thuróczy et  
488 al. (1994) published data on the effects of whole-body RF exposure on the EEG of anesthetized rats.  
489 In that study, the total EEG spectrum increased after 10-min CW exposures at 2.45 GHz, 25 W/kg  
490 BASAR (brain-averaged SAR), but not at 8.3 W/kg. The EEG power in the delta band was augmented  
491 by localized CW exposure of the head at 4 GHz and 42 W/kg (corresponding to a temperature rise of  
492 2 °C). The beta band was increased by exposure at 4 GHz, modulated at 16 Hz and 8.4 W/kg (non-  
493 thermal according to the authors), while the equivalent CW signal did not alter the EEG. One major  
494 limitation of this study was that the animals were anesthetized. These results suggested that a pulsed  
495 RF signal had a greater impact on EEG than CW. In López-Martín et al. (2009), rats were exposed to  
496 a GSM signal and picrotoxin, a GABA ion-channel inhibitor responsible for epileptic seizures.  
497 Exposure to RF at 0.03-0.26 W/kg resulted in a synergistic effect of picrotoxin with GSM that had a  
498 greater impact than CW.

499 This brief review of the literature indicates that RF exposure has indeed been shown to affect the  
500 CNS in humans (mainly EEG) and that results of animal and cell investigations support this  
501 conclusion. This suggests that neuronal networks are targets of RF, although no interaction  
502 mechanism has yet been identified. In that context, *in-vitro* experiments such as those described in  
503 this work, may contribute to identifying the molecular processes involved.

504

## 505 **CONCLUSION**

506 In line with our previous study, we observed *in vitro* an effect of RF exposure on the electrical activity  
507 of rat cortical neuronal networks. We focused on the dependence of this effect on average SAR or E  
508 and the pulsed nature of the RF signal. Both CW and GSM exposures elicited a clear decrease in  
509 burst rate, dose-dependent on SAR or E, but the amplitude of this effect was greater with GSM. We  
510 carefully minimized electrical interference at the electrodes and made sure that the inhibition  
511 observed was not caused by the residual artifact. Mechanisms related to the heating of the culture

512 medium were discounted, in coherence with others results in the literature. However, to date, we have  
513 been unable to elucidate the mechanism behind the observed RF effect on bursting activity in  
514 neuronal networks, but we may conclude that the mechanism is partly nonthermal, and is likely to  
515 involve a direct action of the electric field. In view of the differential effect detected between GSM and  
516 CW, further experiments will test combinations of exposure parameters (amplitude, repetition rate,  
517 and pulse width) to reveal their respective roles in the elicitation of the effect.

518 Further investigation is required to identify specific RF targets at the synaptic or plasma membrane  
519 levels. A comprehensive exploration of the RF action mechanisms on neuronal activity will be  
520 conducted on a pharmacological level. In addition, computational modeling of neuronal networks will  
521 be developed to test the various mechanistic hypotheses.

522

## 523 **GRANTS**

524 This work was funded by the French ANSES agency (2015- EST-15RF-19 MOTUS project).

525

## 526 **DISCLOSURES**

527 No conflicts of interest, financial, or otherwise are declared by the authors.

528

## 529 **AUTHOR CONTRIBUTIONS**

530 N.L., B.V. and I.L. conception and design of research; F.P.G., E.P-H., C.E.K., D.M. and R.R. prepared  
531 cell cultures; C.E.K., D.M., R.R. R.O. and F.C. performed experiments; C.E.K. analyzed data; C.E.K.,  
532 B.V., N.L. and A.G. interpreted results of experiments; C.E.K. and B.V. prepared figures; C.E.K. and  
533 A.G. prepared statistics; C.E.K., B.V. and N.L. drafted manuscript; N.L., B.V., C.E.K. and I.L. edited  
534 and revised manuscript; all authors approved final version of manuscript.

535

536 **REFERENCES**

- 537 Apollonio, F., Liberti, M., Paffi, A., Merla, C., Marracino, P., Denzi, A., Marino, C., D'Inzeo, G.  
538 "Feasibility for microwaves energy to affect biological systems via nonthermal mechanisms: A  
539 systematic approach, (2013) IEEE Transactions on Microwave Theory and Techniques, 61 (5), art.  
540 no. 6478850, pp. 2031-2045
- 541 Bologna LL, Pasquale V, Garofalo M, Gandolfo M, Baljon PL, Maccione A, Martinoia S, Chiappalone  
542 M. Investigating neuronal activity by SPYCODE multi-channel data analyzer. *Neuronal Netw* 23:685–  
543 697, 2010.
- 544 Bolshakov MA & Alekseev SI. Bursting responses of Lymnea neurons to microwave radiation.  
545 *Bioelectromagnetics* 13:119-129, 1992.
- 546 Bolshakov MA, Alekseev SI. Electrical activity dependence of the snail pacemakers on heating rate,  
547 *Biophysics* 31:521-523, 1986.
- 548 Kwon MS and Hämäläinen H. Effects of mobile phone electromagnetic fields: critical evaluation of  
549 behavioral and neurophysiological studies. *Bioelectromagnetics* 32: 253-272, 2011.
- 550 López-Martín E, Bregains J, Relova-Quinteiro JL, Cadarso-Suárez C, Jorge-Barreiro FJ, Ares-Pena  
551 FJ. The action of pulse-modulated GSM radiation increases regional changes in brain activity and c-  
552 Fos expression in cortical and subcortical areas in a rat model of picrotoxin-induced seizure  
553 proneness. *J Neurosci Res* 87: 1484-1499, 2009.
- 554 Loughran SP, McKenzie RJ, Jackson ML, Howard ME, Croft RJ. Individual differences in the effects  
555 of mobile phone exposure on human sleep: rethinking the problem. *Bioelectromagnetics* 33: 86-93,  
556 2012.
- 557 Lustenberger C, Murbach M, Dürr R, Schmid MR, Kuster N, Achermann P, Huber R. Stimulation of  
558 the brain with radiofrequency electromagnetic field pulses affects sleep-dependent performance  
559 improvement. *Brain Stimul* 6 : 805–811, 2013.

- 560 Maccione A, Gandolfo M, Massobrio P, Novellino A, Martinoia S, Chiappalone M. A novel algorithm  
561 for precise identification of spikes in extracellularly recorded neuronal signals. *J Neurosci Methods*  
562 177:241–249, 2009.
- 563 Merla C, Ticaud N, Arnaud-Cormos D, Veyret B, Lévêque P. Real-time RF exposure setup based on  
564 a multiple electrode array (MEA) for electrophysiological recording of neuronal networks. *IEEE MTT.*  
565 59: 755-762, 2011.
- 566 Moretti D, Garenne A, Haro E, Poullétier de Gannes F, Lagroye I, Lévêque P, Veyret B, Lewis N. In  
567 vitro exposure of neuronal networks to the GSM-1800 signal. *Bioelectromagnetics* 34: 571–578, 2013.
- 568 Moretti D. Exposure of neuronal networks to GSM mobile phone signals. PhD Thesis, Université  
569 Sciences et Technologies, Bordeaux, France 2013 (in English) . [https://tel.archives-](https://tel.archives-ouvertes.fr/file/index/docid/949371/filename/MORETTI_DANIELA_2013.pdf)  
570 [ouvertes.fr/file/index/docid/949371/filename/MORETTI\\_DANIELA\\_2013.pdf](https://tel.archives-ouvertes.fr/file/index/docid/949371/filename/MORETTI_DANIELA_2013.pdf)
- 571 Oster S, Daus AW, Erbes C, Goldhammer M, Bochtler U, Thielemann C. Long-term electromagnetic  
572 exposure of developing neuronal networks: a flexible experimental setup. *Bioelectromagnetics* 37:  
573 264-278, 2016.
- 574 Pasquale V, Martinoia S, Chiappalone M. A self-adapting approach for the detection of bursts and  
575 network bursts in neuronal cultures. *J Comput Neurosci* 29:213–229, 2010.
- 576 Perentos N, Croft R, McKenzie RJ, Cosic I. The alpha band of the resting EEG under pulsed and  
577 continuous RF exposures, *IEEE BEM* 60: 1702-1710, 2013.
- 578 Pickard WF and Barsoum YH. Radio-Frequency Bioeffects at the Membrane Level: Separation of  
579 Thermal and Athermal Contributions in the Characeae. *Membrane Biol* 61: 39-54, 1981
- 580 Pikov V, Arakaki X, Harrington M, Fraser SE, Siegel PH. Modulation of neuronal activity and plasma  
581 membrane properties with low-power millimeter waves in organotypic cortical slices. *J. Neural Eng.* 7:  
582 1-9, 2010.
- 583 Pohlert T. The Pairwise Multiple Comparison of Mean Ranks Package (PMCMR), R  
584 package, <http://CRAN.R-project.org/package=PMCMR>, 2014.

- 585 Ramundo-Orlando A. Effects of Millimeter Waves Radiation on Cell Membrane - A Brief Review. J  
586 Infrared Milli Terahertz Waves 31:1400–1411, 2010.
- 587 R Core Team, R: A Language and Environment for Statistical Computing, R Foundation for Statistical  
588 Computing, Vienna, Austria, <https://www.R-project.org/>, 2017.
- 589 Regel SJ, Gottselig JM, Schuderer J, Tinguely G, Rétey JV, Kuster N, Landolt H-P, Achermann P.  
590 Pulsed radio frequency radiation affects cognitive performance and the waking electro-  
591 encephalogram. Neuroreport 18: 803-807, 2007.
- 592 Romanenko S., Siegel P.H.; Wagenaar D.A., Pikov V. Effects of millimeter wave irradiation and  
593 equivalent thermal heating on the activity of individual neurons in the leech ganglion. J. Neurophysiol,  
594 112, 2423–2431, 2014.
- 595 Romanenko S, Siegel PH, Pikov V, Wallace V. Alterations in neuronal action potential shape and  
596 spiking rate caused by pulsed 60 GHz millimeter wave radiation. IEEE 41st International Conference  
597 on Infrared, Millimeter, and Terahertz waves (IRMMW-THz), 2016.
- 598 SCENIHR. Health effects of EMF – Scientific Committee on Emerging and Newly Identified Health  
599 Risks, 2015.
- 600 Schmid MR, Loughran SP, Regel SJ, Murbach M, Bratic Grunauer A, Rusterholz T, Bersagliere A,  
601 Kuster N, Achermann P. Sleep EEG alterations: effects of different pulse-modulated radio frequency  
602 electromagnetic fields. J Sleep Res 21: 50-58, 2012.
- 603 Thuroczy G, Kubinyi G, Bodo M, Bakos J, Szabo LD. Simultaneous response of brain electrical  
604 activity (EEG) and cerebral circulation (REG) to microwave exposure in rats. Rev Environ Health 10:  
605 135-148, 1994.
- 606 Trunk A, Stefanics G, Zentai N, Kovács-Bálint Z, Thuróczy G, Hernádi I. No effects of a single 3G  
607 UMTS mobile phone exposure on spontaneous EEG activity, ERP correlates, and automatic deviance  
608 detection. Bioelectromagnetics 34: 31-42, 2013.
- 609 Van Pelt J, Vajda I, Wolters PS, Corner MA, Ramakers GJ. Dynamics and plasticity in developing  
610 neuronal networks in vitro. Prog Brain Res 147:173–188, 2005.



- 611 Van Rongen E, Croft R, Juutilainen J, Lagroye I, Miyakoshi J, Saunders R, de Seze R, Tenforde T,  
612 Verschaeve L, Veyret B, Xu Z. Effects of radiofrequency electromagnetic fields on the human nervous  
613 system. *J Toxicol Environ Health B Crit Rev* 12:572–597, 2009.
- 614 Wachtel H, Seaman R, Joines W. Effects of low-intensity microwaves on isolated neurons. *Ann NY*  
615 *Academy Sci* 247: 46-62, 1975.
- 616 Wagenaar DA, Madhavan R, Pine J, Potter SM. Controlling bursting in cortical cultures with closed-  
617 loop multi-electrode stimulation. *J Neurosci* 25: 680-688, 2005.
- 618 Xu S, Ning W, Xu Z, Zhou S, Chiang H, Luo J. Chronic exposure to GSM 1800-MHz microwaves  
619 reduces excitatory synaptic activity in cultured hippocampal neurons. *Neurosci Lett* 398: 253-257,  
620 2006.
- 621 Yang L, Chen Q, Lv B, Wu T. Long-Term Evolution Electromagnetic Fields Exposure Modulates the  
622 Resting State EEG on Alpha and Beta Bands. *Clinical EEG and Neuroscience*, 2016.
- 623 Zrenner C, Eytan D, Wallach A, Thier P, Marom S. A Generic Framework for Real-Time Multi-  
624 Channel Neuronal Signal Analysis, Telemetry Control, and Sub-Millisecond Latency Feedback  
625 Generation, *Frontiers in Neuroscience*, 4:173, 2010.

626 **FIGURE CAPTIONS**

627 **Figure 1. A:** Photograph (top), side view (middle), and top view (below) of an open transverse  
 628 electromagnetic cell, showing a circular hole in the TEM cell ground plate to accommodate the MEA  
 629 system. Dimensions in mm: a = 51; b = 100; c = 8; d = 12; h = 1; f = 30; g = 85; l = 14; m1 = 14.5 and  
 630 m2 = 10. **B:** Top: Normalized instantaneous SAR of CW and GSM signals with the same time-  
 631 averaged SAR. Bottom: Normalized instantaneous E of CW and GSM signals with the same time-  
 632 averaged SAR. **C:** Time profile of the exposure protocol: S1 and S2 are control phases before  
 633 exposure; P1 and P2 are control phases after exposure. The E phase corresponds to RF exposure,  
 634 either GSM or CW. In the sham protocol, E corresponds to a sham exposure (no RF).

635

636 **Figure 2. A:** Spontaneous electrical activity of a neuron culture recorded over a 15 min-phase on a  
 637 single electrode, before, during and after exposure to a GSM signal at a SAR of 4.6 W/kg.  
 638 **B:** Corresponding raster plots for each phase showing the analyzed neuronal activity on a group of 22  
 639 electrodes (each one represented in a horizontal line), over the 15 min of recording (i.e. each vertical  
 640 bar representing a spike, each dot representing a burst and each red bar on the bottom of the plot  
 641 representing a network burst implicating the firing of more than 20% of the total electrodes). The  
 642 framed line corresponds to the electrode showed on left.

643

644 **Figure 3.** Box plots with whiskers of normalized Mean Bursting Rate (MBR) for the RF exposed  
 645 cultures, along the five phases (S1, S2, E, P1, P2) of exposure protocol. **A.** Sham exposed cultures  
 646 (n=11). **B.** GSM exposed cultures (n=8) and **C.** CW exposed cultures (n=6) at SAR = 4.6 W/kg. **D.**  
 647 **and E.** Same GSM and CW exposed cultures, shown in B and C respectively, with the MBR being  
 648 averaged for S1, S2 and E,P1 phases, \* p < 0.05, \*\* p < 0.01, p < 0.001\*\*\*, Conover Multiple  
 649 Comparison test.

650

651 **Figure 4.** Variation in the relative decrease in  $R_{\text{MBR}}$  as a function of SAR. Filled and open dots  
652 correspond to experiments using GSM and CW signals, respectively. **A:** All data points. Nonlinear  
653 regression coefficients were 0.67 and 0.77, and  $\text{SAR}_{50}$  were 1.0 and 1.8 W/kg for GSM and CW,  
654 respectively. **B:** Mean points. Nonlinear regression coefficients were 0.85 and 0.89, and  $\text{SAR}_{50}$  were  
655 1.3 and 1.9 V/m for GSM and CW, respectively.

656

657 **Figure 5.** Variation in the relative decrease in  $R_{\text{MBR}}$  as a function of the electric field in V/m. Filled and  
658 open dots correspond to the experiments using GSM and CW signals, respectively. **A:** All data points,  
659 nonlinear regression coefficients were 0.81, and  $E_{50}$  were 6.5 and 22.5 V/m for GSM and CW,  
660 respectively. **B:** Mean points, nonlinear regression coefficients were 0.99 and 0.94, and  $E_{50}$  was 6.5  
661 and 21.3 V/m for GSM and CW, respectively.

662

663 **Figure 6.** Standardized MBR evolution, before, during, and after heating by 1 °C. Filled data points  
664 and curve represent the mean value of MBR (left Y axis), for each phase ( $n= 4$ ) as indicated above  
665 the graph. Grey points and curve represent the temperature elevation (right Y axis) during the  
666 corresponding phases.

667

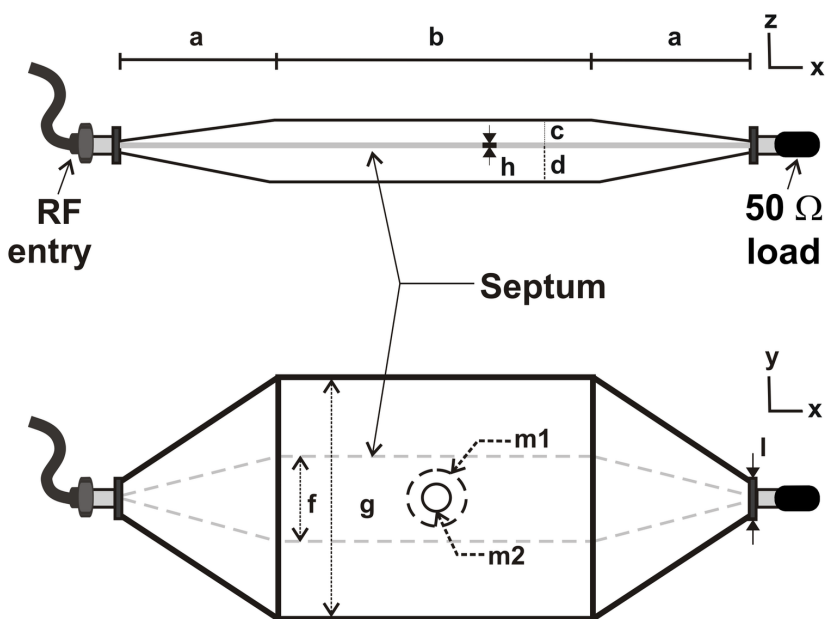
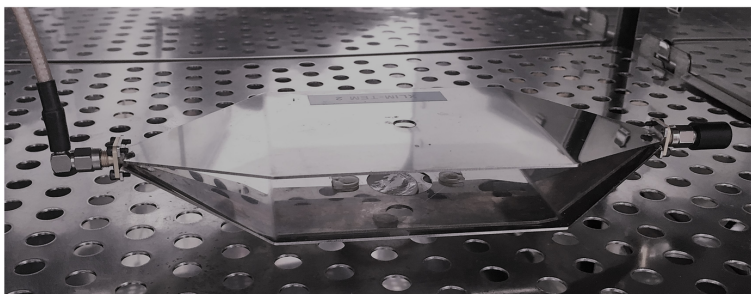
## 668 TABLES

SAR (W/kg)	0 (Sham)	0.01	0.05	0.1	0.3	0.5	0.58	0.92	2.4	4.6	8	9.2
GSM	11	2	1	6	7	0	2	1	6	8	2	6
CW		0	0	6	6	1	2	1	7	6	0	6

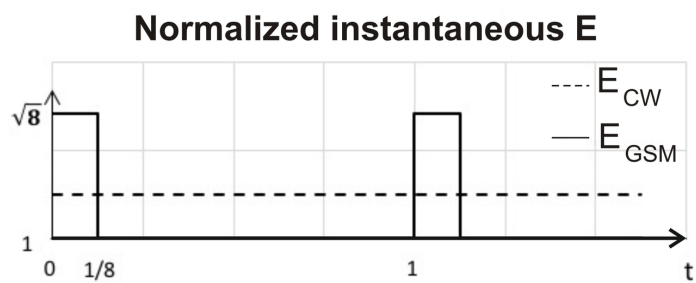
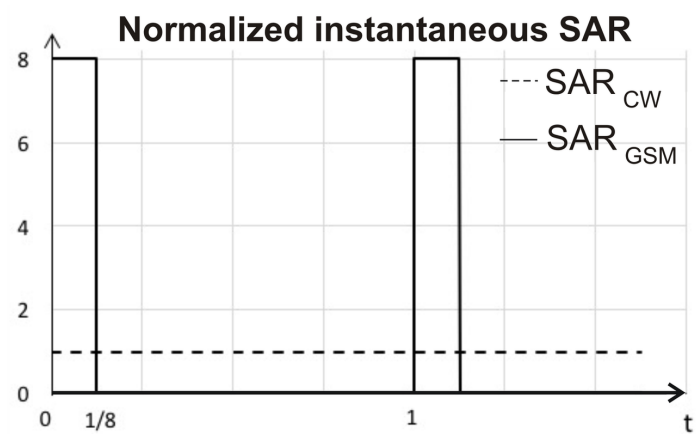
669

670 **Table 1.** List of the SAR levels used and the number of neuronal cultures examined at each SAR, for  
671 GSM and CW signals. The gray columns correspond to the points where at least 6 recordings were  
672 obtained.

A



B

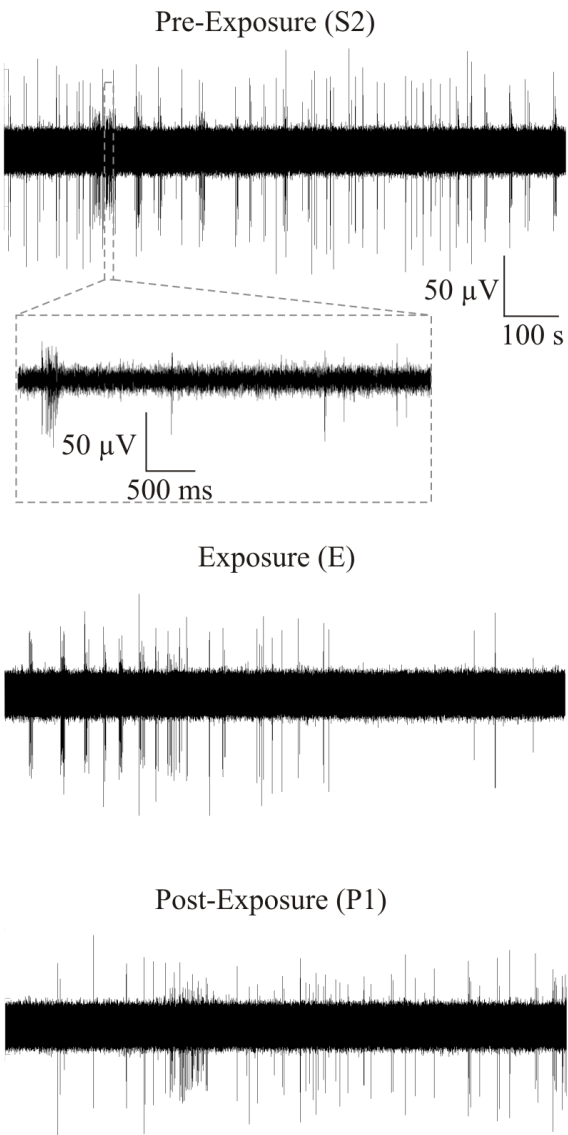


C

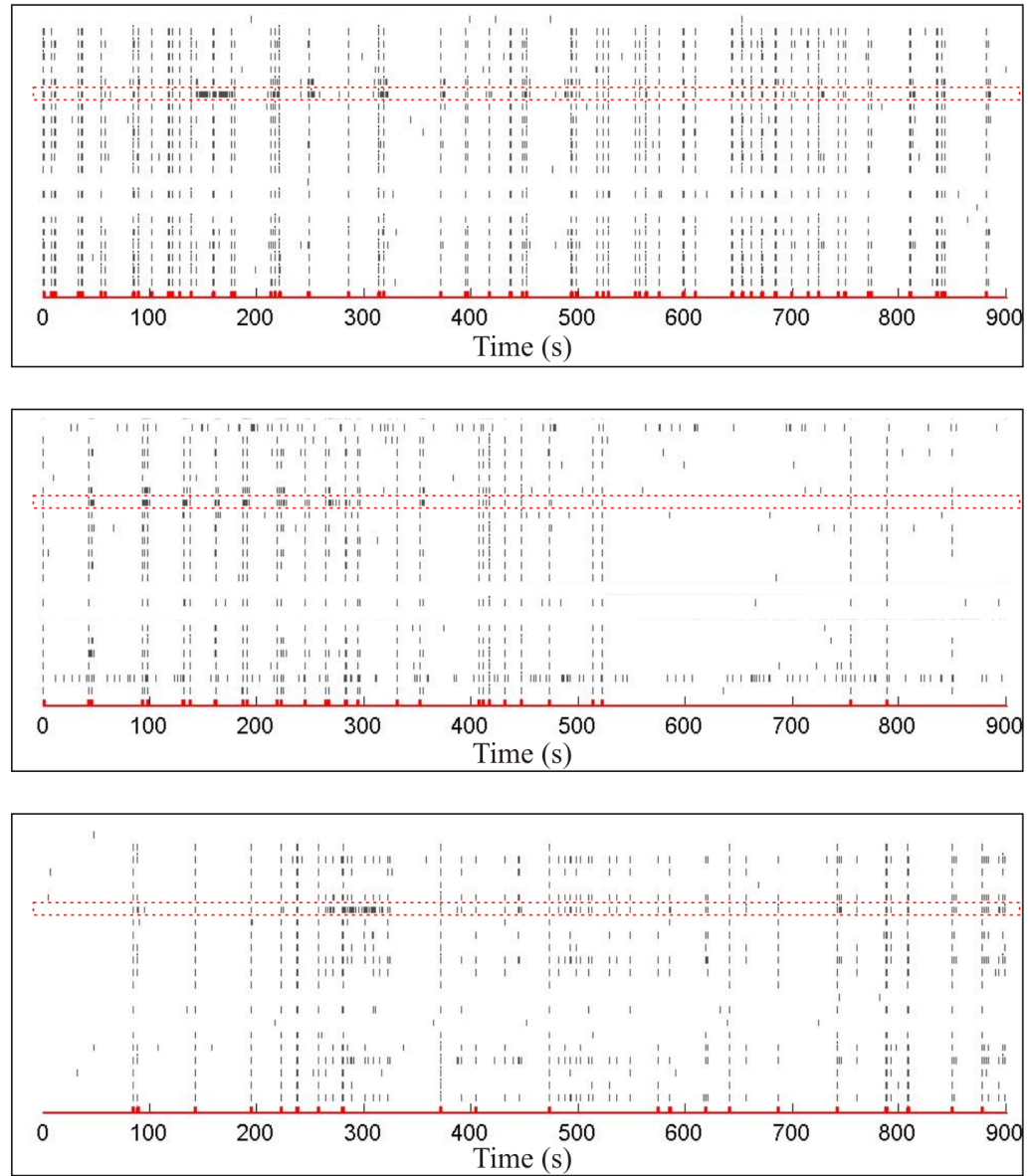
### Exposure Protocol

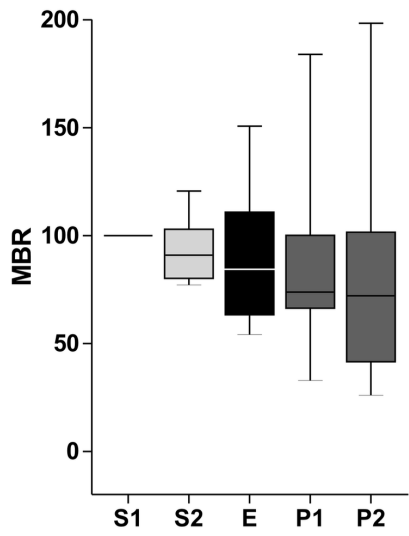
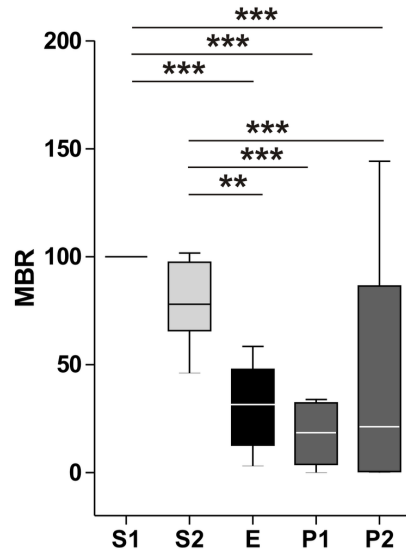
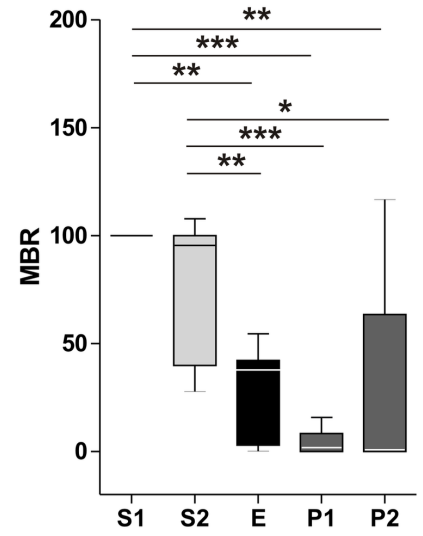
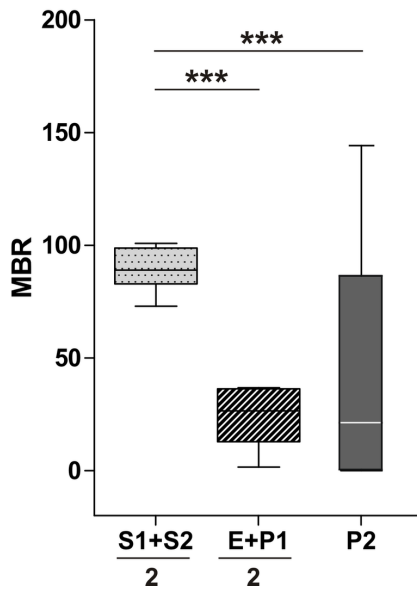
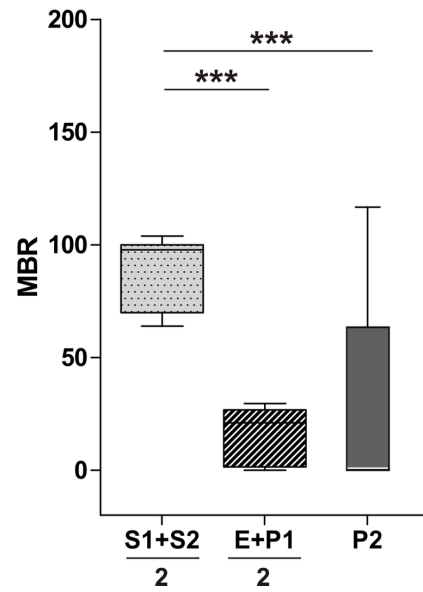
S1	S2	E	P1	P2
15 min	15 min	15 min	15 min	15 min

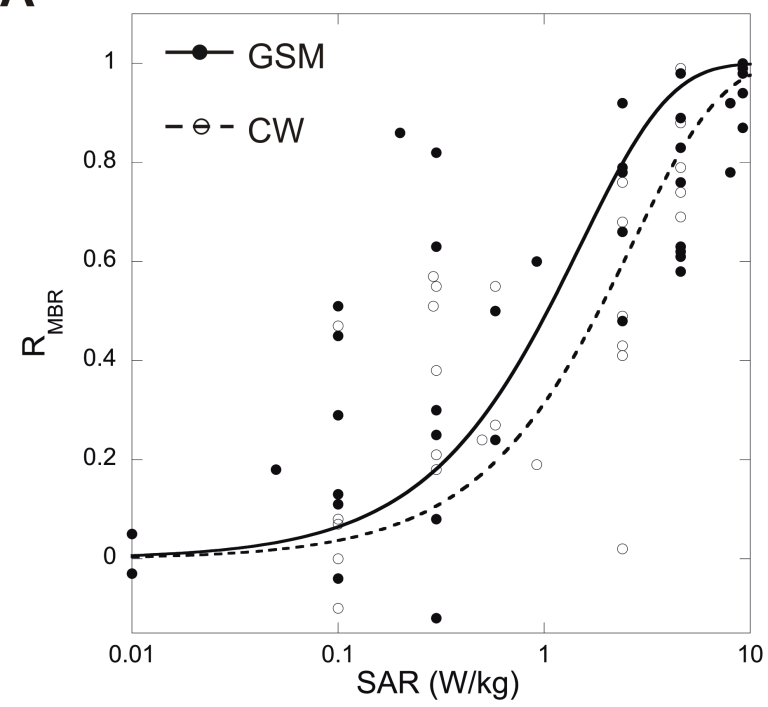
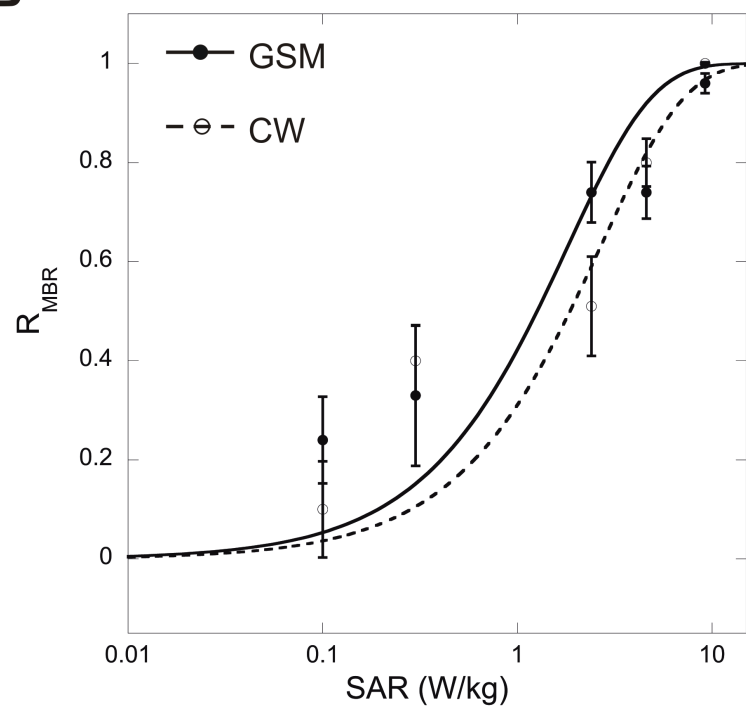
A



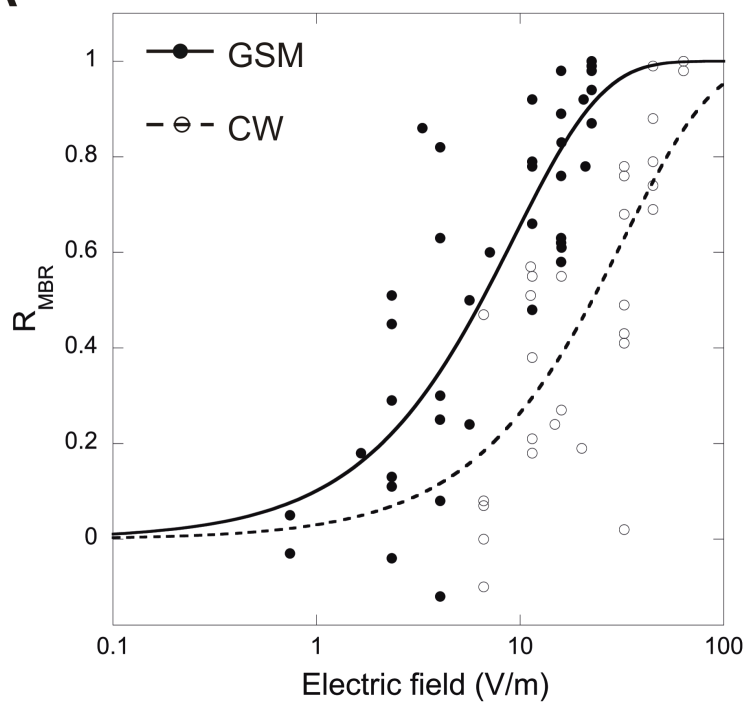
B



**A****SHAM****B****GSM****C****CW****D****E**

**A****B**



**A****B**